water

MDPI

Article

A Mesoporous Faujasite Prepared by Space-Confined Method for Highly Effective Selectivity of Copper Ions

Yi Chen [1], Shiyue Wei [1], Shuai Dong [1], Jinchuan Gu [1,*] and Wenju Jiang [2]

Supplementary Materials

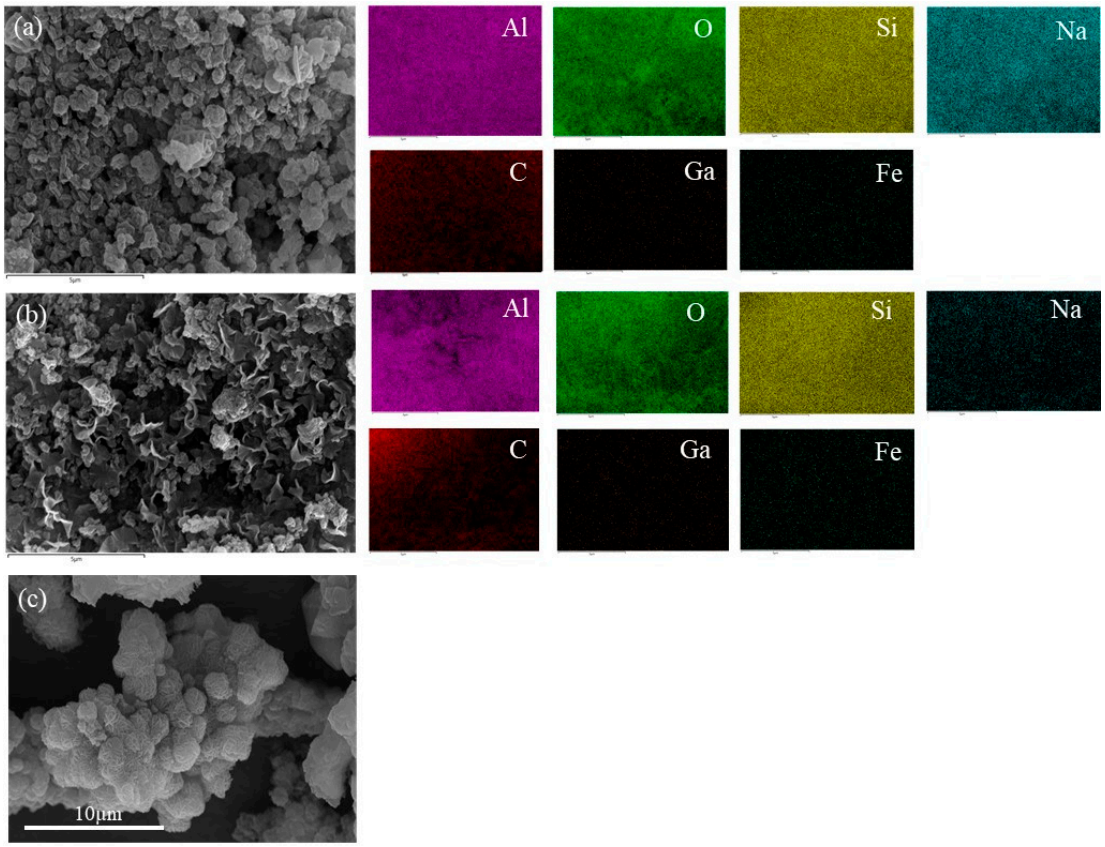

Figure S1. SEM micrograph and the EDS mapping analysis of HN-WSB-Z (a), GZ (b) and the SEM micrograph of Z (c).

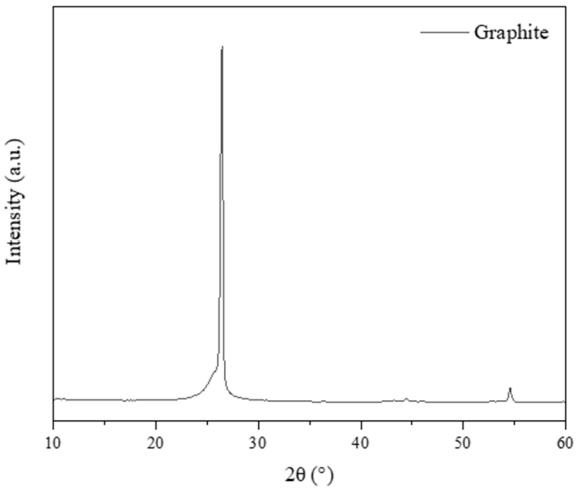

Figure S2. XRD patterns of graphite.

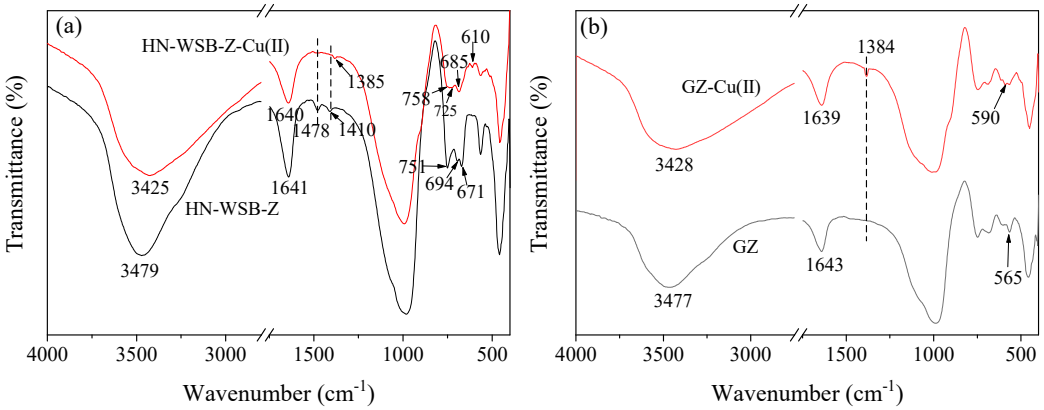

Figure S3. FTIR spectra of HN-WSB-Z and HN-WSB-Z-Cu(II) (a), GZ and GZ-Cu(II) (b).

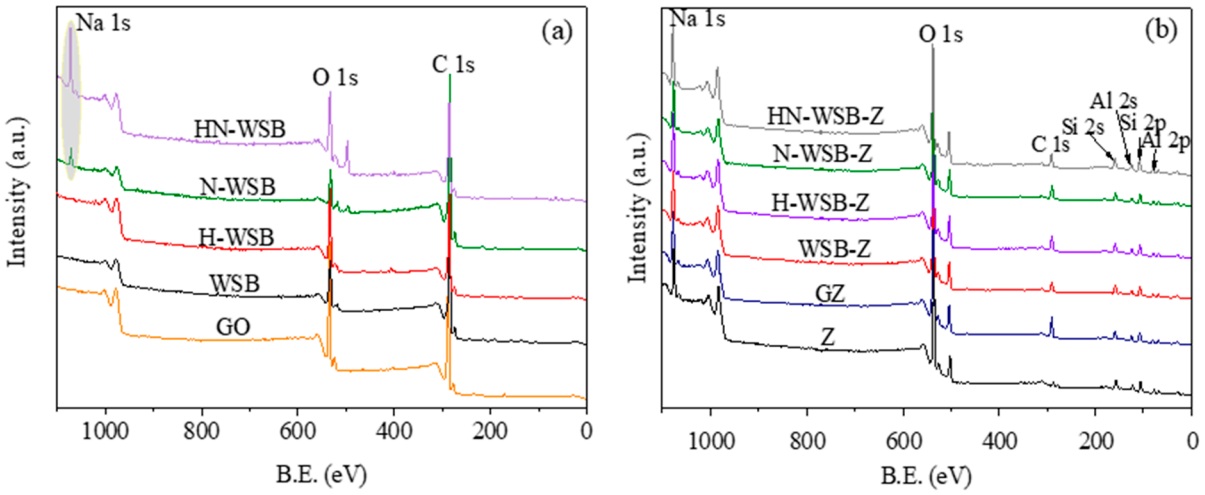

Figure S4. XPS wide-scan spectra of GO and different biochar (a), GO composite FAU, different biochar composite FAUs and pure FAU (Z) (b).

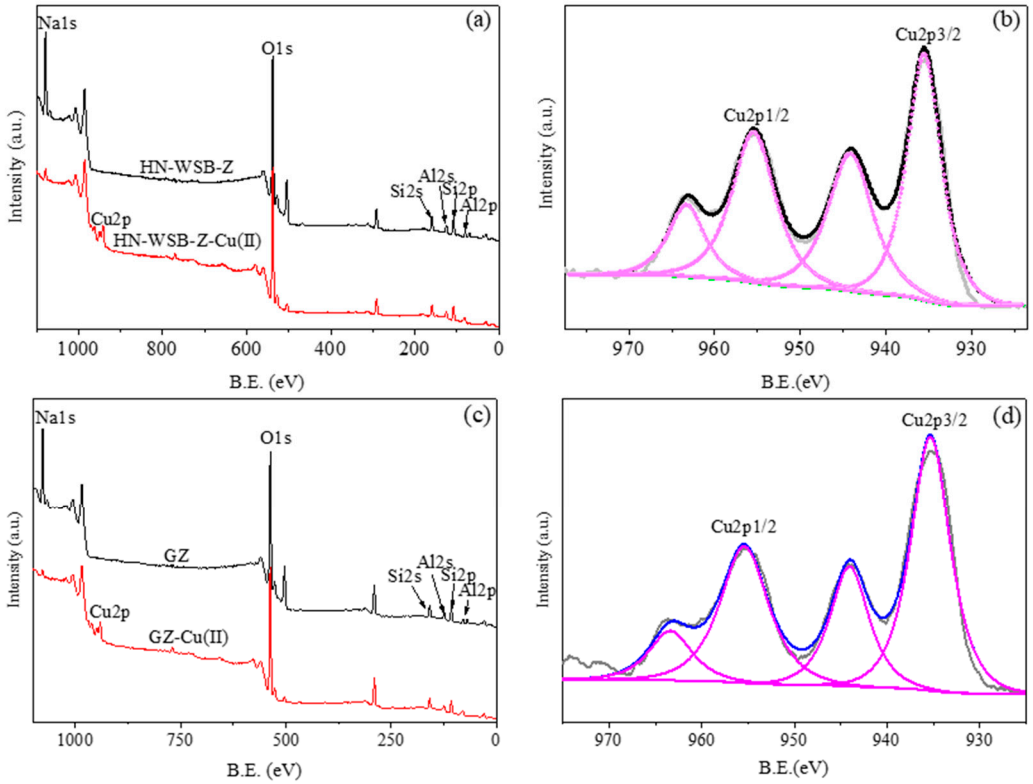

Figure S5. XPS wide-scan spectra of HN-WSB-Z (a) and GZ (c), Cu 2p spectrum of HN-WSB-Z-Cu(II) (b) and GZ-Cu(II) (d).

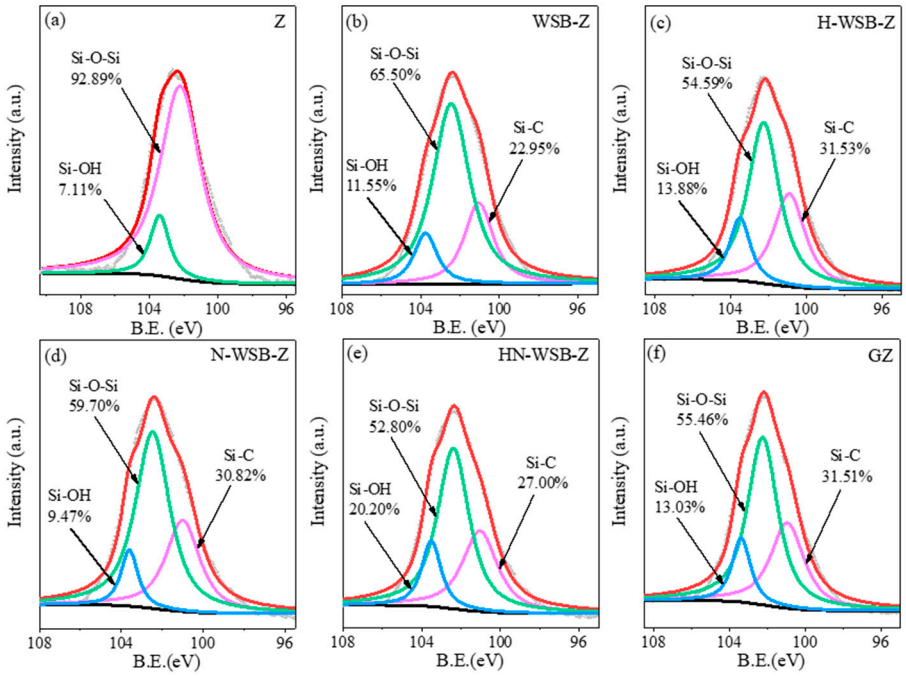

Figure S6. Si 2p spectrum of Z (a), WSB-Z (b), H-WSB-Z (c), N-WSB-Z (d), HN-WSB-Z (e) and GZ (f).

Table S1. The crystallite dimensions of the main lattice planes of different composite FAUs.

Lattice planes	(111)	(642)
Z	450	583
WSB-Z	587	605
H-WSB-Z	592	617
N-WSB-Z	627	631
HN-WSB-Z	526	689
GZ	511	493

Table S2. Kinetics and isothermal adsorption fitting data of HN-WSB-Z and GZ.

	Model	Fitting parameters	GZ	HN-WSB-Z
		$q_{e,exp}$ (mg g^{-1})	93.38	94.74
Isothermal	Langmuir	$q_{e,cal}$ (m g^{-1})	108.68	115.65
		K_L (mL mg^{-1})	2.97	2.63
		R^2	0.9889	0.9927
	Freundlich	K_F ((mg g^{-1})/(L mg^{-1})$^{1/n}$)	71.90	74.27
		1/n	9.47	0.11
		R^2	0.8384	0.8173
Kinetics	Pseudo-1st-order	$q_{e,cal}$ (mg g^{-1})	82.81	85.66
		K_1(min^{-1})	0.22	0.18
		R^2	0.8510	0.8707
	Pseudo-2nd-order	$q_{e,cal}$(mg g^{-1})	95.52	96.50
		K_2 ($\times 10^{-3}$ g (mg min)$^{-1}$)	1.34	1.45
		R^2	1.0000	1.0000

Table S3. α_k^i values of GZ and HN-WSB-Z on multicomponent bivalent metal ions.

.	Cu(II)	Zn(II)	Mn(II)	Ni(II)	Co(II)	Mg(II)
GZ	51.75	0	0	0	0	0
HN-WSB-Z	41.44	0	0	0	0	0